FINAL REPORT

to

HUDSON RIVER FOUNDATION
17 Battery Place
Suite 915
New York, NY 10004

ANTHROPOGENIC ACTIVITY INFLUENCES SEDIMENTARY ENVIRONMENT AND VARIATIONS IN SEDIMENTATION IN THE LOWER HUDSON RIVER ESTUARY

by

Angela L. Slagle
Dept. of Earth and Environmental Sciences
Lamont-Doherty Earth Observatory of Columbia University
Palisades, NY 10964 USA

Graduate Fellowship GF02/05

Abstract

Anthropogenic modifications to the shoreline and body of the lower Hudson River Estuary have been mapped and related to sedimentary environments and sedimentation patterns, by incorporation of historic maps with geophysical data and sediment samples. Modifications studied include urban development of lower Manhattan, as well as bathymetric changes in the estuary between the eighteenth and twenty-first centuries. Development of the shoreline, with piers, outbuilding, and construction of bridges and tunnels, has modified the natural shape of the island of Manhattan by hundreds of meters since early development. Contemporaneous with shoreline modifications, comparison of historic and modern surveys shows changes in bathymetry along lower Manhattan. Shallow water depths (< 11 m), which occupied more than half of the estuary in the 1700s and 1800s, are restricted to the nearshore area in the modern system. Multibeam bathymetry shows an old channel, which hugged the eastern shoreline between the 1700s and 1900s, to be cut off by piers and hardened structures, such as Battery Park City. A newer, wider channel has developed ~ 300 m further to the west, eroding through estuary floor sediments. This reorganization and modern development extends the waterfront of lower Manhattan to the edge of the deep, abandoned channel branch, providing sufficient water depth for river traffic to and from the island.

In the estuarine stretch of the Hudson River between the New York Harbor and Newburgh Bay, detailed patterns of modern sedimentary environment are mapped in regions of human impact. Bridges and tunnels are associated with complex patterns of erosion, scour, and drifts that extend several kilometers from the structures themselves. Pipelines crossing the estuary are commonly areas of local scour, and dump sites are associated with irregular topography, local erosion, and deposition. Areas where the shoreline has been extended and hardened, including piers and docks, are associated with erosional and depositional processes that extend several hundred meters from shore. The spatial impacts of these modifications are not uniform, but influenced by regional conditions, such as surrounding geology and bottom morphology. Patterns of deposition and erosion in the lower estuary may result from estuarine processes acting to establish an equilibrium profile, to balance fluvial, tidal and external influences on the system. Natural erosion events as well as anthropogenic activities, such as hardening of the shoreline and dredging, change the equilibrium profile by removing material, which is followed by enhanced accumulation as the estuary attempts to reestablish equilibrium. Detailed mapping of anthropogenic changes to the estuary through time and the associated variations in bathymetry, sedimentary environment, and sedimentation patterns improves our understanding of human impacts in a natural ecosystem.

1. Introduction

The Hudson River estuary is part of an urban environment that has been greatly influenced by anthropogenic change. While the effects of contaminant releases on sediments, water quality, and ecology have been studied in depth, the effects of human construction and modification of the river bottom are less well understood. Construction of bridges, tunnels, and piers, modification and hardening of shorelines, burial of pipelines and dredging are just a few of the human activities that have taken place during the past century (Coch et al., 1991). These activities are important for the maintenance of the growing population and to support transportation of people and goods within this dynamic region, but they also strongly impact patterns of morphology and sedimentation within the estuary. In the Hudson River estuary, where broad patterns of sediment type, morphology, and erosion/deposition are related to regional factors, including geology and the balance between tidal and fluvial processes, significant variations are also associated with local bedrock, tributaries, and human modifications to the system (Nitsche et al., 2007).

Between 1998 and 2003, the New York State Department of Environmental Conservation (NYSDEC) funded a program to map the bottom of the Hudson River estuary, for studies of sediment transport and habitat classification and to support future management decisions (Nitsche et al., 2005; Bell et al., 2006). As part of this program, multibeam bathymetry, sidescan sonar data, and sub-bottom profiles, in addition to a suite of sediment cores and grabs, were collected for the estuarine stretch of the Hudson River between Troy, NY and the New York Harbor. This study focuses on data collected in the lower estuary, from the Newburgh Bay to the harbor. Specifically, this project (1) details changes in shoreline and bathymetry from the 1700s through the modern setting along the Manhattan stretch of the estuary, (2) investigates the influence of anthropogenic structures on sedimentary environment between Manhattan and Newburgh Bay, and (3) analyzes recent variations in sedimentation patterns from Manhattan to Yonkers, NY.

This research has been presented as a chapter in a doctoral dissertation, “Spatial and Temporal Variability of Sedimentary Processes in the Hudson River Estuary” (Angela L. Slagle, Columbia University, June 2007) and is now being revised as a manuscript, in collaboration with Bill Ryan, Suzanne Carbotte, Frank Nitsche, and Tim Kenna of the Lamont-Doherty Earth Observatory. We hope to submit this work for publication to Marine Geology or Estuarine, Coastal, and Shelf Science in August 2007.

2. Regional Setting

The Hudson River originates in the Adirondack Mountains in northern New York and flows south to its mouth at the Atlantic Ocean. The northern fluvial section is separated by the Troy dam from the tidally-influenced, estuarine section, which extends ~240 km south to the Upper Bay of the New York Harbor. The focus of this study is the lower Hudson River estuary, between Newburgh Bay and the New York Harbor (Fig. 1).

The lower Hudson River estuary is a partially-mixed, mesotidal system, with a tidal range of 1 to 2 meters up to the Troy dam (Olsen et al., 1978). Average water depths range from 15–30 m in the central channel and 1–4 m along the shallow, marginal flats. The estuary varies in width, from the wide Newburgh Bay, Haverstraw Bay, and Tappan

Zee regions to the narrow, bedrock-bound stretches of the Hudson Highlands and Palisades (Nitsche et al., 2007).

The subsurface of the Hudson River estuary shows the effects of glaciation, deglaciation, and postglacial sea level rise (Newman et al., 1969), along with sediment deposition and erosion. The modern lower estuary is dominated by muddy sediments, with the addition of fluvial sand and gravel from the north and marine sand from the south (Olsen et al., 1978; Coch and Bokuniewicz, 1986; Nitsche et al., 2007).

3. Materials and Methods

3.1. Geophysical data

High-resolution multibeam bathymetry was collected for the estuarine stretch of the Hudson River using a SimRad EM-3000 sonar system, with < 1 m horizontal and ~0.3 m vertical resolution. Swath width depends on water depth, so track lines were planned to follow river contours rather than river-parallel. The bathymetry data covers all areas deeper than 5 m water depth, due to the inefficiency of collecting data in shallower waters. The bathymetry data were positioned using DGPS. Raw soundings were corrected for roll, pitch, yaw, tides, and changes in sound velocity, and edited manually to remove spurious soundings. Final depth data were binned into 2 m grids to create a digital elevation model.

Sidescan sonar data were collected using a dual frequency Edge-Tech DF-1000 sonar system, which operates at 100 and 384 kHz. The two frequencies capture different depth intervals in the sediment column, 1–3 cm with 100 kHz and 0.2–1 cm with 384 kHz. Simultaneous with sidescan sonar operations, sub-bottom reflection data were collected using an Edge-Tech 4–24 sonar and XSTAR acquisition system. The sub-bottom sonar was operated with a sweep frequency of 4 to 16 kHz, with a practical vertical resolution of 5–10 cm. Sidescan and sub-bottom data were collected on a grid of north-south and east-west tracks with 80-160 m line spacing. Data were collected using DGPS and shotpoints were corrected to account for the distance separating the GPS antenna from the towed sonars.

3.2. Bathymetric data sources

To investigate differences in bathymetry along the Manhattan stretch of the Hudson River, historic maps and charts provided information with a range of depth units, vertical datums, and accuracy (Table 1). To compare data from different sources, the relative variations in bathymetry over time are evaluated rather than the absolute depth values. Minimal information is available for historic maps from the 1700s (Fig. 2). The 1776 and 1781 maps show characteristic depth soundings only, reported in fathoms, and no vertical datum is recorded. The 1865 map incorporates hydrographic data from surveys between 1854 and 1856. Soundings are expressed in feet up to 18 feet, and in fathoms for all deeper depths, and show depth at mean low water (MLW). This map presents characteristic soundings only, selected from a larger dataset to accurately represent the estuary bottom. The 1906 map is based on multiple data sources, including surveys by the Coastal and Geodetic Survey in 1885 and 1889, with corrections from the NYC authority in 1903, and the U.S. Corps of Engineers in 1907 (Fig. 3). The 1924 map is based on a

U.S. Engineers hydrographic survey from 1924. All soundings from 1903 and 1924 are expressed in feet at MLW. The 1998 nautical chart shows hydrographic data collected between 1978 and 1996 and reports soundings in feet at mean lower low water (MLLW). Multibeam bathymetry from our NYSDEC-funded surveys is reported in meters, with depths relative to NAVD88. These water depths shown are ~1 m greater than depths reported relative to MLLW displayed on modern NOAA nautical charts.

3.3. Geographical information system (GIS) analysis

Archived and new bathymetry data were incorporated in a geographical information system (GIS) to document changes in shoreline and bathymetry during the last several centuries. Historic maps of the Manhattan area from 1766, 1776, 1781, and 1865 were obtained from the U.S. Library of Congress and navigational charts from 1906, 1924, and 1998 were obtained from the National Oceanic and Atmospheric Administration's Office of Coast Survey (NOAA OCS) collection. Using ArcMap software, designed by Environmental Systems Research Institute, high-resolution digital images of maps and charts were geometrically transformed, which transfers map features or coordinates from the scanned units into projected coordinates such as Universal Transverse Mercator (UTM) coordinates (Chang, 2006). Through geometric transformation, the digitized maps can be aligned with other data layers, including the modern bathymetry data from our NYSDEC-funded surveys. Historic maps and charts were georeferenced, using latitude/longitude where available and common topographic or structural features with known geographic coordinates as control points. Maps were transformed using an affine transformation, which allows rotation, translation, skew, and differential scaling on a rectangular object but preserves line parallelism (Pettofrezzo, 1978). Using ArcMap, all historical maps and modern data layers were projected into a common reference system, WGS (World Geodetic System) 1984 UTM Zone 18N, to align all layers.

In order to evaluate changes in the morphology of the estuary floor, georeferenced maps of historic bathymetry were created by contouring individual soundings, creating shapefiles using ArcMap, and color-coding them according to depth (Fig. 3). For all historic maps, soundings were binned based on depth ranges, choosing a range of depths for each map that is roughly equivalent for the different depth units reported (fathoms, feet, and meters).

Interpretive maps of sedimentary environment were developed for the southern reaches of the estuary (between Manhattan and the Tappan Zee area), based on GIS analysis of multibeam bathymetry, sidescan sonar, and sub-bottom data. The method is described in detail by Nitsche et al. (2005), Bell et al. (2006), and Slagle et al. (2006); the interpretation for this study was carried out in conjunction with the work of these authors, whose sedimentary environment maps are used for the northern reaches of the study area (between the Tappan Zee and Newburgh Bay regions). Three broad categories of sedimentary environment were established to classify processes dominating the estuary floor: deposition, erosion, and dynamic (Table 2). Depositional environments are identified by a smooth estuary floor, low sidescan backscatter, and an acoustically-transparent, surface sediment layer in sub-bottom data. Erosional environments are characterized by an irregular or rough estuary floor, high backscatter values in sidescan data, and truncated sedimentary layers in sub-bottom profiles. Dynamic environments include regions where bedforms, such as sediment waves or flow-parallel features, are

imaged in bathymetry and regions where sidescan and sub-bottom data show evidence of localized erosion and deposition, often associated with obstacles on the estuary floor. Detailed sedimentary environment sub-categories are described in Table 2.

3.4. Sediment sample collection and measurements

More than 600 sediment samples were collected as part of the NYSDEC-funded project, between the New York Harbor and Newburgh Bay from 1998 to 2003, to characterize the estuary floor and to ground truth acoustic data. Grab samples provide information on surface sediments, while 1- to 2-m-long gravity cores allow us to examine deeper sediments. An additional gravity core (EM05-GC-02), collected north of the George Washington Bridge (GWB) in 2005, is also included in this study.

Physical properties, including gamma density, magnetic susceptibility, and p-wave velocity, were measured at 1-cm intervals for whole sediment cores using a GEOTEK multi-sensor core logger. Cores were split lengthwise, photographed, and described to document color, structure, and composition. Surface sub-samples of grabs and cores were analyzed for grain size composition, using a sonic sifter with standard sieves for the coarse fraction (>63 μ) and Sedigraph system for the fine fraction (≤ 63 μ). Selected cores were sub-sampled for loss-on-ignition (LOI), measured following the method of Dean (1974) to assess relative changes in organic content of sediments, and gamma counting, to measure ^{137}Cs and ^{210}Pb activities following methods detailed elsewhere (Olsen et al., 1981; Cutshall et al., 1983; Feng et al., 1998). Activities of total ^{137}Cs and ^{210}Pb were measured via gamma spectroscopy of the 46.5 and 661.6keV photopeaks, respectively; excess ^{210}Pb activity was determined by subtracting the activity of its ^{214}Bi parent from the total activity. All activities are reported as pCi (picocuries) per kilogram dry weight and confidence limits are one standard deviation unit. Activities are corrected to the date of sample collection.

3.5. Sedimentation rates

^{137}Cs has been dispersed globally by atmospheric testing of nuclear weapons beginning in 1952, with fallout reaching significant levels in the Northern Hemisphere in 1954 and peaking in 1963. Profiles of ^{137}Cs provide age markers for sediments accumulated over the last ~50 years. Although we have reasonable ^{137}Cs profiles, we are not certain that our data capture the complete profile back to 1954 (Fig. 9). Accumulation rates calculated from excess ^{210}Pb activity (see below) suggest that ^{137}Cs profiles are truncated by an unconformity in cores, which is supported by abrupt changes in other sediment properties (lithology, density, LOI; Fig. 11). For this reason, we do not use ^{137}Cs to calculate sedimentation rates or to assign absolute ages.

^{210}Pb is produced as atmospheric fallout from the decay of ^{222}Rn gas, but also found in small quantities in most soils as part of the ^{238}U decay series. Much of the ^{210}Pb in shallow sediments is derived from atmospheric ^{222}Rn, while much of the ^{210}Pb (and ^{222}Rn) in deeper sediments is derived from ^{226}Ra in the water. Excess ^{210}Pb in sediments over that in equilibrium with the *in situ* ^{226}Ra in sediments provides information about sediment ages and accumulation rates over the last 100–150 years. Excess ^{210}Pb profiles for our cores show some scatter or disturbance, but generally exhibit a monotonic decrease in the log of activity for sediments above an unconformity in cores, which can be interpreted as steady state accumulation and radioactive decay (Fig. 10). While

activities may be low (between 0 and 2700 pCi/kg), they are similar to previous studies in the Hudson and other estuaries (e.g. Feng et al., 1998; Klingbeil and Sommerfield, 2005; Church et al., 2006). In order to obtain estimates of accumulation rates where data showed a log-linear trend, we used the constant flux model (Krishnaswamy et al., 1971), fitting an exponential curve to the excess ^{210}Pb versus plotted against cumulative mass.

4. Manhattan development: 1766 to 2003

4.1. Early development of the city of New York (lower Manhattan)

To track the development and urban layout of the city of New York, early maps of Manhattan, ranging over a century (1766 to 1865), were compared (Fig. 2). The earliest map of New York, from 1766, shows the city occupying the southwest tip of the island of New York, called Manhattan by the "native savages" (text from 1766 map shown in Fig. 2). The city was located at the confluence of the North or Hudson's River and the East or Sound River. An organized grid of streets appears at the southwestern tip of Manhattan. The earliest streets, closest to the Battery, are organized in an east-west, north-south grid. The beginnings of further development show in a change of street orientation, as the orthogonal grid changes to a northwest-southeast trend. "Broad Way", the southernmost part of the modern Broadway, leads northeast from Fort George at the Battery, terminating in an area of higher terrain with a fresh water lake. Several main routes extend further northward, providing access to the more rural areas of the city, including "Bowry Lane", equivalent to the modern Bowery.

In the 1776 and 1781 maps, development of the urban grid has extended further north, along the western edge of Manhattan and in the central and eastern part of lower Manhattan along "the Bowry". The new streets fit the northwest-southeast trend, rather than the earlier north-south grid. Several additional crossroads develop in the north, extending perpendicular to the main artery of the Bowry Lane, trending in an east-west direction. They provide access to the rural eastern coast of lower Manhattan. Local streets extend from the fresh water lake in the developed portion of Manhattan to the surrounding rural area and more secondary roads appear in the northern areas. Individual rural tracts appear to be larger than those of the previous decade. Both the 1776 and 1781 maps show regions of (modern) Brooklyn and Queens, which are almost entirely rural with very few roads.

By 1865, a dense, orthogonal grid of streets has been established across Manhattan, extending from the Hudson to the East River, from the Battery to as far north as the modern 155th street, across the estuary from Fort Lee, NJ. The earliest streets from the 1700s, at the southwest tip of Manhattan, maintain the same east-west orientation in the 1865 map. Development along the western shore of Manhattan, along the Hudson River, continued roughly east-west, but central and northern Manhattan development built up in a northwest-southeast orientation that is roughly parallel to the long axis of the island. Main roads from the earliest maps, including Broadway and Bowry Lane, remain in their northeast-southwest orientation and extend northward as thoroughfares to northern Manhattan. However, the east-west trending roads that crossed the Bowry in the 1770s and 1780s have been replaced by northwest-southeast trending streets. The lake in lower Manhattan has been filled in and developed by 1865 and there are no remaining rural

spaces south of 155th street. Both Brooklyn and Queens, which were entirely rural in earlier maps, are also completely developed in a dense grid of roads by 1865. The orientation and density of streets shown in the 1865 map is equivalent to the configuration of New York City today (Fig. 3).

4.2. Shoreline modifications

The 1766 map of New York shows a coastline characterized by both natural and man-made features. The western edge of Manhattan has an irregular, slightly rippled shoreline that appears to conform to the geology of the island. The Battery consists of several constructed features, including Fort George, reinforcing the location and shape of the shoreline at the southern tip of the island. Piers and docks (30-75 m long) are constructed along the shore in the developed areas of the city, particularly along the southern edge of the island on the East River. A small section of the northwestern edge of lower Manhattan is also developed with piers in the 1760s.

In 1776 and 1781, more slips and piers are developed along the waterfront at the southern edge of Manhattan. Several pre-existing piers appear to have been lengthened up to 100 meters. A shipyard is also established along the southern shore. The "Brookland Ferry" is established along the north shore of the modern Brooklyn, to provide the closest access across the East River to Manhattan. Maps from 1776 and 1781 show some of the natural features of Manhattan, including the narrowing and change of angle of the island to the north. These maps also identify the salt marshes along the eastern shore of Manhattan and show a curving bay where the island narrows. Several small streams or inlets are shown within the bay and all along the eastern shore of the island.

By 1865, 50 to 200 m long piers are developed along the entire western and southern shorelines of lower Manhattan. Piers appear along much of the shore of the modern Brooklyn, in the East River and also toward the New York Harbor. The Battery, at the southern tip of Manhattan, has been extended by ~200 meters toward the harbor. As the island of Manhattan is urbanized, many of the natural features of the shoreline are obscured by development. Comparison of the 1865 shoreline to maps of the 1700s shows that the western shoreline of lower Manhattan has been extended out toward the Hudson River (Fig. 2). Much of the natural irregularity of the shoreline has been built out and smoothed by waterfront development. The island is substantially built out at the northern extent of the 1700s maps, near the area marked Greenwich, where the Manhattan bends to the east. In this area, Manhattan has been widened by between 150 and 500 meters. Along the eastern shoreline, the salt marshes and bays have been filled in and developed, widening the island by as much as 400 meters and straightening the natural shape of the shore. The lateral growth of Manhattan constitutes an estimated 17% increase in surface area of the island below 25th Street (the northernmost extent of pre-1800s maps) between 1781 and 1865.

The entire shoreline of Manhattan has been artificially smoothed and straightened between 1865 and the 1900s (Fig. 3). In the 1906 map of Manhattan, piers along the western shore have been lengthened to 200-300 m. Piers now extend from the shore in all areas of lower and middle Manhattan. The island has been widened by up to 400 meters, north of 23rd Street, where Manhattan bends to the east. The Brooklyn suspension bridge

now extends from Brooklyn to Manhattan, across the East River, at the site of the Brookland Ferry of the late 1700s. Governor's Island, in the harbor just south of Manhattan, is being extended by infilling. By 1924, Governor's Island has doubled in area. The 1924 shoreline is similar to the 1906 shoreline, but in the ~20 elapsed years between maps, the Manhattan, Williamsburg, and Queensboro bridges were constructed across the East River.

Between the 1924 and 1998 maps, both the Holland Tunnel (1920-1927) and the Lincoln Tunnel (1934-1935) were constructed as highway tunnels beneath the Hudson River, connecting lower and central Manhattan to New Jersey. In the 1960s and 1970s, a 90 acre community known as Battery Park City was planned for development at the southwestern tip of Manhattan. A 1600 m stretch of shoreline that had formerly been piers was built out into the Hudson River and infilled with material excavated for the construction of the World Trade Center and other projects. In the 1998 map, Battery Park City is shown extending 200 to 300 meters into the Hudson off southwestern Manhattan. The eastern shore of Manhattan is also shown to be built out into the East River by ~200 m in the 1998 data, through infilling areas formerly occupied by piers. The modern shoreline, shown in the 2002-2003 map, is consistent with the development from 1998.

4.3. Morphology and bathymetry patterns

Comparing historic maps that document water depths with modern soundings and bathymetric data reveals changes in the bathymetry of the Hudson River estuary along Manhattan that are contemporaneous with anthropogenic modifications to the shoreline. Historic maps from the 1700s have limited depth information, intended not for navigation purposes, but to provide a general sense of the shape of the river bottom. On the 1766, 1776, and 1781 maps, depth information is shown only for the southern tip of the island of Manhattan (Fig. 2). These maps show that the deep areas ($\geq$ 11 m) fall within a few hundred meters of the western shore of Manhattan, indicating that the channel hugged the coast. The deepest depth (~14.5 m) is shown close to the island, off the northwestern part of the Battery. At that time, the width of the Hudson between New Jersey and lower Manhattan ranged from 2–3 km.

By 1865, the island of Manhattan has been widened and the distance across the estuary to New Jersey has decreased. More depth data are provided in the 1865 map, but still only a representative set of soundings convey the shape of the estuary. Contouring of the 1865 soundings shows that the channel continues to run along the western shore of Manhattan, as suggested in earlier maps (Fig. 3). The deepest depths in the 1865 map ($\geq$ 20 m) lie just off the western corner of central Manhattan where the island bends, along the southwestern edge of lower Manhattan, and in the New York Harbor east of Governor's Island. The western half of the estuary is relatively shallow, with most depths falling below ~ 11 m (6 fthm).

More recent sounding data is shown on a fairly dense grid on nautical charts issued by the U.S. Coast and Geodetic Survey and the National Oceanic and Atmospheric Administration, from the 1900s through the modern period (Fig. 3). Contouring 1906 soundings shows the features of bottom morphology in more detail than earlier maps. Along northern and central Manhattan, the channel (14-20+ m deep) appears closer to the New Jersey shore. At the bend in the island, around 23rd St., channel orientation switches

to the east side of the Hudson. As shown in earlier maps, the 250- to 350-m wide channel continues to run closely along the west shore of lower Manhattan. The Hudson also appears to have deepened by 2-3 meters, with shallowest depths (≤ 32 ft or ~10 m) shown closer to the New Jersey shoreline than in the 1865 map. This is consistent with work of Klingbeil and Sommerfield (2005), which suggests that the accretionary nature of the Holocene channel in the lower estuary shifted to an erosional state during the late 1800s, perhaps associated with shoreline development.

Soundings on the 1924 map show a similar pattern to those from 1906. Along lower Manhattan, the channel continues to hug the western shore of the island and the channel depth range is similar (14-20+ m). Deepest depths continue to be found in the channel where the island and estuary change orientation and east of Governor's Island. One notable difference in 1924 bathymetry is a 350 m stretch of shallower depths in the channel, about 1 km north of the Battery. The 1924 chart shows four ferry docks along this stretch of the Manhattan shoreline. Frequent ferry traffic may be responsible for resuspending sediment from the estuary floor and causing infilling in this area. The 1924 channel off lower Manhattan is also 50-100 meters narrower than the 1906 channel.

By 1998, the morphology of the estuary channel has become less coherent. Along central Manhattan, the channel is shown to occupy the center of the estuary, rather than the western edge, as shown in previous maps. Much of the estuary has deepened to a uniform depth of ~14 m (46 ft) compared to earlier maps, which showed a greater distribution of depths between 0 and 14 m. There is still evidence of a channel along the western shore of lower Manhattan, but the channel has shallowed considerably (by ≥ 3 meters). The deepest portion of the channel is broken up by an 850 m stretch of shallower area, a few km north of the Battery, likely related to the construction of the Holland Tunnel beneath the estuary. The shallowest areas of the estuary (≤ 10 m) are confined to narrow strips close to the shorelines of New York and New Jersey, and just off the Battery. Battery Park City, constructed in the 1970s, has been built out to sit right at the edge of the older, deep channel (15-20 m) along southwestern Manhattan. In fact, much of the waterfront of lower Manhattan sits at fairly deep water depths for this part of the Hudson (~14 m), which would provide sufficient depth for deep-keeled boats to easily access the area. At this time, bathymetric data shows the development of a deeper channel where the Hudson meets the harbor, toward the center of the estuary. The newer channel runs along the central and western portions of the estuary, more than 800 meters offshore of lower Manhattan.

Modern bathymetric data, collected in multibeam surveys between 2002 and 2003, show the continued development of the newer, western channel off lower Manhattan (Fig. 3, Fig. 4). The western channel extends almost 2 kilometers further north from the harbor than in the 1998 map. The new channel is separated from the older, eastern channel by a shallower ridge, imaged with ~ 5 meters of relief in multibeam data. The ridge extends nearly 5 kilometers north of the Battery, separating the old channel from the new. The eastern channel no longer extends uniformly along the western shore of lower Manhattan. It is cut off by shallowing at the Holland Tunnel and by the construction of Battery Park City, and isolated from deep areas of the harbor by the increasingly shallow (< 10 m) region off the Battery.

Based on these maps, the most significant change is the reconfiguration of the main channel associated with modification of the lower Manhattan shoreline. From historic maps up through 1924 data, the channel consistently occupies the eastern edge of the estuary, with a thalweg 50 to 200 meters off the shore of Manhattan (Fig. 3). The channel of the early 1900s is 200 to 300 meters in width and connects directly to the deepest part of the harbor. In 1998 and 2002-2003 data, much of the estuary off lower Manhattan has deepened (> 14 m) and the channel system has become more complex (Fig. 3, Fig. 4). The older, eastern channel has narrowed to ~ 150 meters in width, with depths ranging from 16.5 to 20 m, and is isolated from other deep areas of the estuary. Multibeam bathymetry and cross-estuary sub-bottom profiles show a ridge, at ~ 15 m depth, that separates the old channel from a newer channel to the west (Fig. 4d). The new, western channel ranges from 350 to 550 meters in width. Deepest depths (17-18.5 m) lie between 300 and 500 meters off the coast of Manhattan. Sub-bottom profiles within the newer channel reveal truncated sedimentary layers intersecting the estuary floor, indicating the erosion of bottom sediments to form the new channel (Fig. 4c). It appears to have been the extension, infilling, and hardening of the Manhattan shore associated with the 1970-1980 construction of Battery Park City that ultimately led to the abandonment of the old, eastern channel and erosion of the new western channel.

5. Modern sedimentary environment, Manhattan to Newburgh Bay

Integrating geophysical data, including multibeam bathymetry, sidescan sonar data, and sub-bottom profiles, with sediment data from cores and grabs in a GIS, we develop a series of process-based sedimentary environmental classes to describe the Hudson River estuary (Nitsche et al., 2004; Bell et al., 2006; Slagle et al., 2006). High-resolution data provides the potential for detailed mapping of modern patterns and variations of sedimentary environments along the estuary floor. Significant variations in sedimentary environments are associated with areas of human impact on the estuarine system (Nitsche et al., 2007).

5.1. Sedimentary environment of lower Manhattan

Since the 1700s, the Manhattan stretch of the estuary has undergone urban development, expansion and hardening of the natural shoreline with piers and docks, and widening of the island by infilling and out-building (Fig. 2, Fig. 3). These anthropogenic modifications correspond to changes in bathymetry and estuary morphology, but also to complex patterns and variations in sedimentary environment.

The shorelines of the southern reaches of the Hudson are dominated by anthropogenic structures, including piers on both New Jersey and New York banks. The estuary floor in this area is characterized mainly by erosion and dynamic environments (Fig. 4b). Multibeam bathymetry shows a wide swath of irregular structures covering the broad channel floor (Fig. 4a), which are imaged as erosionally-truncated, dipping sedimentary layers in sub-bottom data (Fig. 4c). The erosion may be the result of restricted flow caused by the expansion and hardening of the shoreline along lower Manhattan. Dynamic scour, evidenced by rough topography in multibeam data and high sidescan backscatter, is shown on the western banks of the channel. A field of dynamic sediment waves extends down into the harbor area just off the Battery, along the wall of the western

channel. A narrow flow-parallel ridge separates the modern, western branch of the channel from the older, eastern channel. Truncated layers are imaged in sub-bottom data on the western flank of the ridge and dynamic scour appears on the eastern flank. East of the ridge, in the older channel, a thin swath of truncated sedimentary layers are seen in sub-bottom data.

A local area of dynamic scour and drifts is associated with the Manhattan pipeline crossing, south of the Holland Tunnel (Fig. 4b; Table 4). Where the Holland Tunnel crosses beneath the estuary, erosion dominates the estuary floor and areas of dynamic scour are shown along the shore. South of Union City, NJ, the channel deepens locally and becomes dominated by dynamic scour and sediment waves. Erosion, evidenced by truncated reflections in sub-bottom data, continues to occur along the banks of the channel. As the estuary bends to the east, a field of irregular topography, showing truncated layers in sub-bottom data, occupies the middle of the channel. This area is flanked by a complex pattern of dynamic scour and sediment waves. Construction of the Lincoln Tunnel, which crosses beneath the estuary at this bend, may be responsible for the complex dynamic and erosive patterns of the estuary floor in this area (Table 4). A thin drape in sub-bottom data, indicating a depositional environment, covers much of near-shore pier area along Manhattan and most likely results from sediment trapping and accumulation associated with the piers of New York and New Jersey.

5.2. Anthropogenic structures from Manhattan to Newburgh Bay

Anthropogenic modifications to the shoreline of the Hudson River extend far beyond the development of the New York Harbor and lower Manhattan, throughout the estuarine and fluvial portions of the system. The focus of this study is the estuarine section of the Hudson, between Manhattan and Newburgh Bay, the upstream extent of the salt wedge. Mapping sedimentary environments through this area reveals local variations in patterns of deposition, erosion, and dynamic processes similar to those described along lower Manhattan, associated with the presence of anthropogenic structures, including bridges, pipeline and cable crossings, dumping grounds, and other examples of extension and/or hard structures along the shore (Table 3, Table 4).

Bridges crossing the Hudson River estuary are typically associated with erosion and dynamic sedimentary environments that can extend up to several kilometers north and south of the structures themselves (Fig. 4b, Fig. 5, Table 4). At the George Washington Bridge, 17 km north of the Battery, dynamic scour dominates the channel and margins, while drifts extend south of the bridge (Fig. 5a). A narrow (~75 m) region of erosion hugs the east bank, just beneath the bridge. The Tappan Zee Bridge (41 km from the Battery), with its close-spaced supports, is associated with a narrow, east-west trending region of dynamic scour that extends ~4200 m across the estuary, from shore to shore (Fig. 5b). Beginning about 1 km from the western shore, dynamic scour is accompanied by the development of dynamic drifts or “bridge ribbons” extending more than 3000 m, up- and down-stream of the bridge (Table 4). These flow-parallel ribbons have significant topography in multibeam data (up to 2m). Areas of the channel on either side of the bridge show evidence of truncated layers in sub-bottom data, indicating erosion of the floor. A region of sediment waves extends north and south of the bridge. The local sedimentary environment of the Newburgh-Beacon Bridges (Fig. 5c) is similar to that of the Tappan Zee Bridge. Sediment waves extend north of the bridge and broad regions of

the estuary floor are scoured on either side of the bridge, increasing from 700 m wide north of the bridge to 1400 m beneath it. Bridge ribbons form to the north and south, extending up to 4000 m, parallel to estuary flow (Table 4). For all three bridges in the study area, sedimentary environment maps show that bridge ribbons are wider and longer in the high-energy, deep channel than on the shallow margins (Fig. 5; Table 4).

Pipelines crossing the estuary are associated with a range of dynamic sedimentary environments, often appearing very locally. South of the Holland Tunnel, a narrow band of scour and drifts occur along the path of a Manhattan pipeline crossing (Fig. 4b; Table 4). A similar localized region of scour and drifts occurs along the pipeline crossing just north of the Lincoln Tunnel, extending ~10 m north and south of the pipeline itself. A region of sediment waves is disrupted by the Piermont Pier pipeline crossing (Fig. 5b). In multibeam bathymetry, the pipeline has little topographic expression along the western channel wall, but it is associated with a deep trench across the channel floor. Dynamic scour, evident in sidescan backscatter, is seen along the pipeline's path across 1700 m of the estuary. Dynamic streaks extend north and south of the pipeline along the western channel wall, stretching up to 2000 m in the flow-parallel direction (Table 4).

Dumping grounds are associated with regions of dynamic debris, areas with erosive and depositional features associated with the irregular morphology of the dump sites (Fig. 5a). The discontinued dumping ground north of the George Washington Bridge is an area of complex morphology in multibeam bathymetry, including small mounds and irregular terrain. Often these areas show signs of scouring and sediment tails around individual features.

A range of additional anthropogenic modifications have been made to the lower Hudson River estuary, including bulkheading (or hardening) the shore (Coch et al., 1991). A few specific examples of hardening of the shore north of Manhattan are shown in Figure 5a and 5b. Ross Dock, a modern picnic area that extends out into the Hudson north of the George Washington Bridge, was built on sunken barges and other landfill. The ~50 m by 250 m picnic area is associated with a mix of dynamic sedimentary environments, including sediment waves, drift and scour that stretch up to 300 m across the estuary and more than 800 m along the estuary (Fig. 5a; Table 4). An arcuate region erosion and nondeposition several kilometers long is shown of the end of the Piermont Pier, built in the 1840s, 38 km from the Battery (Fig. 5b; Table 4). Sub-bottom data shows eroded sedimentary layers and multibeam data shows rugged topography in the region west of the pier. A confined region of deposition appears directly northwest of the pier. It is likely that changes in local hydrodynamics associated with construction of the pier resulted in the sedimentary pattern of this region.

We find that human interventions in the lower estuary are associated with distinct changes in morphology, bathymetry, and variations in sedimentary environment. The zones of impact surrounding these anthropogenic structures and modifications differ from region to region. For example, the George Washington Bridge impact is spatially less than that of the Newburgh-Beacon Bridges, which extends up to 4 km along the estuary (Fig. 5b-c; Table 4). The impact of the pipeline crossing south of Piermont Pier is larger than the impact of the pipelines crossing the estuary in lower Manhattan, by roughly two orders of magnitude in the along estuary dimension. The modification of the shoreline by construction of Battery Park City appears to have had an even larger impact, leading to a

reorganization of the channel system off lower Manhattan. Our data suggest that the spatial impacts of human modification are influenced by regional conditions. Nitsche et al. (2007) distinguish eight significantly different sections of the Hudson River Estuary and show that regional changes in morphology, sediment type, and sedimentary environment correspond well with changes in surrounding bedrock, and tributary input. Such regional variations may also be critical influences on the spatial impacts of human modifications to the estuary.

6. Recent sedimentation, Manhattan to Yonkers

To investigate patterns of sediment accumulation over the last 100-150 years, data from cores sampling 1-2 m of sediment were incorporated with geophysical data from the stretch of the estuary between Manhattan and Yonkers, NY (Fig. 6). The southern portion of this straight, relatively narrow section of the estuary is developed with piers and docks along the New Jersey shoreline and the George Washington Bridge (GWB) crosses this stretch of the estuary. North of the bridge, the Palisades Sill dominates the western shoreline, while highways and train tracks run along the eastern banks. The natural channel occupies eastern side of the estuary in this stretch and shallow, marginal flats (or shoals) stretch from the channel to the western bank. Previous work on sedimentation in this area has documented the accumulation of a cohesive channel and shoal system (Klingbeil and Sommerfield, 2005), sediment transport in an estuarine turbidity maximum in the stretch 10-25 km from the Battery (ETM; Geyer et al., 1998; Geyer et al., 2001), and seasonal patterns of deposition west of the channel (Woodruff et al., 2001).

6.1. Sedimentation on the marginal flats

Sidescan sonar data from this area, collected between 2001 and 2003, show moderate to high backscatter within the main channel and lower backscatter along the marginal flats west of the channel (Fig. 6). This pattern is consistent with a previous sidescan survey conducted in this area in 1998 (Woodruff et al., 2001). A narrow band of low sidescan backscatter south of the GWB is coincident with the dredged Weehawken-Edgewater Channel. This channel runs along the west side of the estuary and was maintained at ~9 m water depth by the Army Corps of Engineers up through ~1994 (Woodruff et al., 2001; Fountain, 2003). Low sidescan backscatter over the dredged channel has been linked to recent deposition of high-porosity mud, infilling the dredged channel (Woodruff et al., 2001). A similarly distinct low backscatter region, with a larger, more irregular shape than the dredged channel, is imaged on the marginal flats north of the GWB (Fig. 6). This region extends 19 km along the estuary and varies in cross-estuary width, from 10s of m beneath the GWB to 1 km north of the northern tip of Manhattan. Our maps of sedimentary environment interpret these two low backscatter regions to be dominated by deposition. In contrast to the low backscatter marginal flats in the vicinity of the GWB, the marginal flats further north in the Tappan Zee area are characterized by moderate sidescan backscatter and interpreted as dynamic, erosional environments (Carbotte et al., 2004; Nitsche et al., 2005; Slagle et al., 2006).

Sub-bottom data from the Manhattan-Yonkers area show a distinct surface layer coincident with the low-backscatter region north of the GWB (Fig. 7a). The layer ranges

from ~10 to 70 cm in thickness, assuming a constant velocity of 1500 m/s for estuarine sediment to convert two-way travel time to depth. The water-sediment interface in this region is relatively smooth, in contrast to the rough character of the estuary floor in the channel. The surface layer is acoustically transparent, unlike deeper sediments where internal horizons are common, and in some places, partially masks acoustic imaging deeper in the sedimentary column. South of the GWB, a surface layer with a somewhat different acoustic character is imaged coincident with the dredged Weehawken-Edgewater channel (Fig. 7c). The lateral boundaries of this layer are sharp and it completely masks the imaging of deeper sediments. The lack of penetration beneath this layer is consistent with bubble scattering and this zone is interpreted to consist of gas-charged sediments infilling the dredged channel (Klingbeil and Sommerfield, 2005). North of the low-backscatter region, sub-bottom profiles show a rough bottom with sub-bottom horizons truncated at the estuary floor on the marginal flats, indicative of erosion (Fig. 7b; Slagle et al., 2006). Sub-bottom data shows no evidence of an acoustically-transparent surface layer in this area.

The most notable feature of sediment cores from the low backscatter region north of the GWB is the distinct color stratification, characterized by a layer of dark black mud (30-70 cm thick) that changes abruptly to an olive brown sediment (Fig. 8a). Both layers contain laminations of silt and sand. The contact between these layers is characterized by finger-like intrusions of dark black mud (4-20 cm long) into the olive brown sediment below. Thickness of the black mud layer measured in individual cores corresponds well to estimates of the acoustically transparent layer imaged in sub-bottom profiles. A thin layer (1-20 cm) of water-rich sediment is present at the top of most cores in this low backscatter region and, in description and location, closely resembles a seasonal deposit of high porosity, olive brown mud observed in this area by Woodruff et al. (2001). In contrast, cores from the channel contain layers of shell material and anthropogenic debris such as brick dust and slag but lack the distinct color stratification of the low backscatter marginal flats. Cores from the east bank of the estuary have alternating intervals of black and brown sediment with gradual color transitions (Fig. 8b). Cores from the dredged Weehawken-Edgewater Channel have yet a different appearance, characterized by brown, highly-laminated sediment (Fig. 8b). A water-rich surface layer is present in some of the east bank and Weehawken-Edgewater cores, also likely to be associated with the deposit observed by Woodruff et al. (2001).

Sub-bottom penetration of ^{137}Cs activity in cores from the low backscatter region provides some age information, to constrain when the dark black mud and surface layer were deposited. Measurable activity extends 40-50 cm below the surface within black sediments, decreasing below the level of detection beneath the black–olive brown boundary, suggesting that sediments above the boundary postdate 1954 (Fig. 9). The abrupt color change and accompanying loss of ^{137}Cs activity across the boundary may indicate an erosional origin for the boundary surface, which may truncate the ^{137}Cs profile. As a result, we do not use ^{137}Cs activity to assign absolute ages or calculate sedimentation rates. Excess ^{210}Pb profiles from two cores in the low backscatter area (LWB1-16, EM05-GC-02) show a reasonable linear trend in the surface and black mud layers, indicating a steady rate of sediment accumulation (~1.1 g/cm^2/yr). There is some scatter of data that may indicate a disturbance in EM05-GC-02, but generally the curves are good fits to the data. Excess ^{210}Pb decreases rapidly below the black–olive brown

boundary (Fig. 10). The drop in activity across the boundary is also consistent with an erosional interpretation.

Photographs and profiles of ^{137}Cs, gamma density, and LOI from cores within the low backscatter region show good agreement between the distinct color stratification and changes in geochemical and physical properties in the vicinity of the GWB (Fig. 11). Measurable ^{137}Cs extends through the surface and black mud layers, but decreases below the black–olive brown boundary (Fig. 9, Fig. 11). Sediment accumulation rates, from excess ^{210}Pb, indicate that sediment above the boundary has been deposited at a steady rate over the last ~30 years for cores LWB1-16 and EM05-GC-02. Density profiles show abrupt increases across the boundary, with higher densities typical of older, more compact sediments in the deepest olive brown sediment. LOI, where measured, decreases below the boundary, indicating lower organic carbon content in olive brown sediment. This trend is repeated in LOI data from an additional core in the low backscatter area (not shown). Together, these data support the interpretation of the boundary as an unconformity, representing an event or period of sediment erosion or non-deposition that may have taken place ~1970.

6.2. Origin of sedimentation patterns

Similarities in sidescan backscatter, location, and sub-bottom characteristics initially suggested that the low backscatter region north of the GWB and the Weehawken-Edgewater Channel may have comparable anthropogenic origins, as areas of sediment infilling following dredging activities. Many estuarine systems are extensively dredged to maintain sufficient water depths for harbors and shipping channels and studies have shown dredging activities to induce rapid sedimentation (e.g. Olsen et al., 1981; Nichols and Howard-Strobel, 1991; Olsen et al., 1993). The low backscatter region south of the GWB bridge has been linked to infilling of the dredged Weehawken-Edgewater Channel (Woodruff et al., 2001; Fountain, 2003). The Weehawken-Edgewater Channel was constructed in 1920 to provide commercial access to deep draft terminals along the New Jersey shoreline and dredged semi-annually by the U.S. Army Corps of Engineers until terminals closed and dredging ceased in 1994 (Fountain, 2003). However, there are no Army Corps records of dredging activity in the low backscatter region north of the GWB (ACE personal communication) to suggest that the recent black mud layer observed in sediment cores is post-dredging infill.

More detailed investigation of the distribution, sub-bottom character, and sediment properties in the northern low backscatter region does not support a dredging origin for the unconformity. The dimensions of the low backscatter region are irregular and it occupies a large portion of the marginal flats north of the GWB (~8.2 km^2; Fig. 6), which is incongruous with planned dredging activity when compared to the well-documented Weehawken-Edgewater dredged channel, which occupies a very regular, narrow strip of the marginal flats (~1.8 km^2). The acoustically-transparent surface layer in the northern low backscatter region corresponds to a distinct sediment layer, based on good agreement between thicknesses measured in individual cores and sub-bottom profiles that transect core locations (e.g. Fig. 7a). Sediments of a different acoustic character are imaged below the surface layer in this region, consistent with a lithology change below the black mud layer. This contrasts with the appearance of a surface layer and lack of deeper acoustic penetration over the known dredged channel, which is likely due to gas presence within

sediments (Hagen and Vogt, 1999; Woodruff et al., 2001) rather than a change in sediment properties.

The thickness of the black and surface layers in cores, along with the changes in ^{137}Cs activity, excess ^{210}Pb activity, density, and LOI, were used to estimate the amount of material accumulated above the unconformity. The spatial distribution of these sediments was guided by the low backscatter region in sidescan sonar data and the presence of distinctive acoustically transparent surface sediments in sub-bottom profiles (red polygon; Fig. 6). Based on a minimum thickness of 30 cm, the volume of sediment overlying the unconformity is approximately 2,500,000 m^3. The estimated volume of sediment overlying the unconformity increases to approximately 4,100,000 m^3 when the mean thickness (50 cm) of the surface and black muddy layers in sediment cores is used. This volume is more than twice the documented volume of sediment removed to construct a channel in Haverstraw Bay to the north in 1960-1961 (~1,300,000 m^3, from Army Corps records). The spatial distribution, the amount of material present above the level of the unconformity, and the lack of commercial requirement for a dredged shoal in the area argue against an undocumented dredging project of such magnitude as the origin of the low sidescan backscatter region and underlying unconformity.

A natural erosional event or series of events, mostly likely predating 1970, may be the origin of the unconformity observed in sediments of the low backscatter area north of the GWB. High flow events, such as river floods, have been shown to enhance the erosive power of ebb tidal currents (Geyer et al., 2001) and records from the Hudson indicate several high-magnitude flooding events in the last ~50 years that may be linked to our unconformity north of the GWB (Klingbeil and Sommerfield, 2005). Another plausible source of erosion of the area is tidal flow elevated by storm surge and records show five great surges in the Hudson since 1950 (Klingbeil and Sommerfield, 2005). Using sub-bottom data, Klingbeil and Sommerfield (2005) mapped a seismic reflector (R1) north of the GWB, which they interpreted as an erosion surface created by one or multiple erosion events occurring ~1954. Based on lateral extent, acoustic character, and age estimates, it is likely that our unconformity is the same surface as the R1 reflector of Klingbeil and Sommerfield (2005). Our unconformity is characterized by a distinct color change in cores, while the R1 reflector is described as overlain by a 1-2 cm lag of anthropogenic debris that is absent in our cores; this discrepancy may be an artifact of the density of core sites. Measurable ^{137}Cs activity below the depth of R1 in cores suggests that it may closer in age to our unconformity (~1970) than the interpreted age of 1954 (Klingbeil and Sommerfield, 2005). Higher resolution dating and more detailed sediment analysis may provide more insight into the specific timing and origin of the unconformity, but our sediment cores provide clear evidence of an erosional event followed by deposition on the marginal flats at some point prior to 1971.

Accumulation of the black mud and water-rich surface sediment overlying our unconformity is likely due to the focusing and trapping of elevated suspended sediment in the region north of the GWB. Most estuaries exhibit such a region, the estuarine turbidity maximum (ETM), where the flow regime focuses suspended sediment into a particular area, usually near the landward end of the salinity intrusion (Olsen et al., 1978; Nichols and Howard-Strobel, 1991; Geyer, 1993; Jaeger and Nittrouer, 1995). An ETM is found in the Hudson, 10-20 km north of the Battery, and numerical modeling studies predict a zone of sediment trapping just north of the GWB (Geyer et al., 1998).

Sedimentation rates on the flats underlying the ETM are reported to be among the highest in the estuary (Olsen et al., 1981). Although decadal scales of accumulation in the Hudson ETM have not been established, recent studies show a large amount of spatial variability in sedimentation and a distinct seasonal deposit in the low backscatter region north of the bridge which may ultimately lead to the accumulation we observe (Feng et al., 1998; Woodruff et al., 2001; Traykovski et al., 2004).

Although the unconformity and overlying sediment deposit we observe may not be a direct result of anthropogenic activity such as dredging, the interplay of erosion and deposition leading to these features on the marginal flats may be linked to human intervention in the lower Hudson. Detailed analysis of bathymetric changes between 1939 and 1999/2002 in the Yonkers stretch of the Hudson by Klingbeil and Sommerfield (2005) reveals recent changes in sedimentation conditions, including accretion in the low backscatter region north of the GWB and erosion of the channel, and a ~10% loss of native estuary surface area. The study of Klingbeil and Sommerfield (2005) suggests that the decrease in cross-sectional area due to shoreline development in the lower estuary resulted in erosion in the channel to reestablish equilibrium cross-sectional area, and speculates that such subaqueous erosion constitutes a significant internal source of sediment. The local source of sediment from ongoing subaqueous erosion of the modern channel may be focused and trapped in the ETM, perhaps leading directly to the relatively rapid accumulation of sediment overlying our unconformity north of the GWB.

7. Maintaining equilibrium

Changes in estuary morphology and bathymetry, local variations in sedimentary environment, and patterns of deposition and erosion may be governed by physical processes acting to establish or maintain the estuary floor in dynamic equilibrium with respect to river discharge, tidal currents, and wave activity in the estuary. The concept of an equilibrium profile was first applied in the early 1900s to explain erosional and depositional features in stream and beach profiles, and has since been applied to coastal bays and estuaries (Olsen et al., 1993). Any change in the long-term energy field of an estuary must be compensated in the equilibrium profile through erosion or deposition, maintaining a balance between accumulation and erosion in association with fluvial and tidal actions.

Although McHugh et al. (2004) contend that the Hudson River estuary north of Haverstraw Bay has reached a state of equilibrium, based on sediment bypassing, fine-scale observations of spatial and temporal variations in erosion and deposition patterns suggest that a long-term equilibrium surface has not been established everywhere in the lower Hudson River estuary. The alternation of erosion events, which may lead to sediment unconformities, with depositional periods over decades or even centuries suggests that the estuarine system is continuing evolving to maintain a dynamic equilibrium. This is consistent with the observations of Klingbeil and Sommerfield (2005), who propose a model for the marginal flats (or shoals) beneath the Hudson ETM that requires both regular accretion and phases of erosion by flooding or storm surges, in order to maintain a uniform depth.

We find that man's intervention in the lower estuary acts as an anthropogenic analogue to natural events that disrupt the processes acting to establish an equilibrium profile. Infilling of the eastern channel branch off lower Manhattan, following hardening and building out of the Manhattan shoreline in the 20th century appears to account for change in the hydrodynamics and cross-sectional area of the lower estuary. The contemporaneous erosion of a new channel, along the western side of the estuary, is required to compensate for the change in profile. This interpretation is supported by observations of channel erosion in the region of the GWB, linked to hardening of the shoreline and loss of surface area in the lower estuary (Klingbeil and Sommerfield, 2005). Spatial patterns of sedimentary environments on the modern estuary floor also reflect localized regions of dynamic and erosional processes associated with anthropogenic structures, such as the flow-parallel sediment drifts and scoured regions mapped around the Tappan Zee Bridge. Dredging activities in the harbor, Weekhawken-Edgewater, and Haverstraw Bay areas of the Hudson, as well as in other estuaries, have cut channels far below natural equilibrium depths, inducing rapid sediment and associated contaminant accumulation to compensate (Olsen et al., 1993; Woodruff et al., 2001; Fountain, 2003).

8. Summary and conclusions

Studies suggest that there is considerable spatial and temporal variability of deposition and erosion within the lower Hudson River estuary and these variations are influenced by changes in river flow (Feng et al., 1998; Geyer et al., 1998; Woodruff et al., 2001), climate (Carbotte et al., 2004), sea level (Slagle et al., 2006), bedrock and tributary input (Coch and Bokuniewicz, 1986; Nitsche et al., 2007), as well as human intervention (Olsen et al., 1981; Bokuniewicz and Coch, 1986; Olsen et al., 1993; Klingbeil and Sommerfield, 2005; Nitsche et al., 2007). In an urban system such as the Hudson River estuary, anthropogenic activities invariably influence the natural environment, sometimes in ways that have not been predicted in advance. However, advancing technology and innovative techniques provide a more detailed picture of the complex urban estuary and its response to anthropogenic changes. Incorporation of historical data with modern geophysical and sediment data in a GIS allows for a detailed assessment of changes in shoreline and bathymetry, as well the associated variations in sedimentary environment and sedimentation patterns, in the estuarine section of the Hudson River.

Although New York City has evolved as an urban area since its early settlement as a British colony, certain aspects of its development have followed the plan established by the 1700s. The orientation of streets laid out as early as 1766 is maintained in the urban layout of the modern city. The 1766 street plan involved an east-west trending grid at the southwest tip of Manhattan and along the Hudson shore, but as urban development expanded to the north, a northwest-southeast grid was established in central and eastern Manhattan. This pattern seems to follow the constraints of Manhattan geology, as the island narrows slightly and bends to the east, from south to north. Several of the main roads of the 1760s, including Broad Way and Bowry Lane, serve as major routes through the 1860s and continue to be well-established in the modern city.

The anthropogenic development of the Manhattan section of the Hudson River has changed the shoreline and bathymetry in the area since the 1760s. Comparison of historic maps with modern charts show a widening of Manhattan by as much as 500 meters, as land is built out from the natural coast of the island, first with piers, then with hardened structures like Battery Park City. The construction of bridges and tunnels around the island is another means of modification to the area. Historic maps also reveal changes in bathymetry that are contemporaneous with anthropogenic development of Manhattan. The shallow water depths (< 10 m), which occupied the western half of the estuary through the early 1900s, are confined to the very near-shore areas in 1998 and 2003 maps. As early as the 1700s, the main channel along Manhattan was shown to hug the western shore of the island before entering the New York Harbor. By the mid-1900s, the western channel has narrowed, and in modern multibeam bathymetry, the old channel has been overtaken by waterfront development. The old channel is cut off by piers and the construction of Battery Park City and shoaled, most likely due to the change in hydrodynamics, while a new channel has eroded along the central and eastern portion of the estuary (~ 300 m to the west) to accommodate flow. In the modern Manhattan stretch of the Hudson River estuary, the waterfront has been extended out to the edge of the abandoned channel, providing deep-water access for deep-keeled boats and river traffic. The removal of cross-sectional area by outbuilding of the western shore of Manhattan is equivalent to the removal of material by natural erosive events. The estuary system compensates for anthropogenic activity by enlarging cross-section in one area of the estuary and providing a new supply of sediment for deposition in another.

In addition to bathymetric variations, anthropogenic modifications to the estuary are associated with variations in sedimentary environment. Complex patterns of dynamic and erosional environments, mapped from high-resolution geophysical data, are shown in areas of human impact in the estuarine portion of the Hudson River. Bridges and tunnels are commonly associated with erosion, scour, and flow-parallel drifts that may extend for several kilometers to the north and south of the structures themselves. Scour is often found locally where pipelines are laid across the estuary. Dumping grounds are areas of complex morphology, with scouring and sediment tails around individual bottom features. Anthropogenic structures that extend and harden the shore, such as piers and docks, are commonly associated with erosion where they perturb estuarine flow and deposition and infilling where they inhibit flow. The spatial impacts of these structures appear to be related to the variations in regional environment, in addition to the nature of the modification. Our data suggest that the modifications to the Manhattan shore, which reorganized the channel system off lower Manhattan prior to 1998, had a larger impact on hydrodynamic flow and sediment transport than any of the other structures evaluated in this study.

Patterns of deposition and erosion can be governed by physical processes acting to establish a sediment surface in dynamic equilibrium with respect to river outflow, tidal currents, and wave action. Natural erosion events, such as floods and storm surges, as well as anthropogenic activity, such as shoreline hardening, outbuilding, and dredging, remove material from the estuary, which may result in the migration of depocenters and regions of erosion to compensate for the change in the equilibrium profile. Spatial and temporal variations in sedimentation suggest that the lower Hudson River estuary has not established a long-term equilibrium surface.

Detailed mapping of temporal and spatial changes to the bathymetry, sedimentary environment, and sedimentation patterns improves our understanding of the impact of human modifications to a natural system. Understanding and modeling these relationships is a critical step toward predicting the effects of future anthropogenic and natural changes on this system

References

Bell, R.E., Flood, R.D., Carbotte, S.M., Ryan, W.B.F., McHugh, C.M.G., Cormier, M., Versteeg, R., Bokuniewicz, H.J., Ferrini, V., Thissen, J., Ladd, J.W. and Blair, E.A., 2006. Benthic habitat mapping in the Hudson River Estuary. In: J.S. Levinton and J.R. Waldman (Editors), The Hudson River Estuary. Cambridge University Press, Cambridge; New York, pp. 51-64.

Bokuniewicz, H.J. and Coch, N.K., 1986. Some Management Implications of Sedimentation in the Hudson-Raritan Estuarine System. Northeastern Geology, 8(3): 165-170.

Carbotte, S.M., Bell, R.E., Ryan, W.B.F., McHugh, C.M.G., Slagle, A., Nitsche, F.O. and Rubenstone, J., 2004. Environmental change and oyster colonization within the Hudson River estuary linked to Holocene climate. Geo-Marine Letters, 24(4): 212-224.

Chang, K.-t., 2006. Introduction to Geographic Information Systems, Third Edition. McGraw-Hill, New York.

Church, T.M., Sornmerfield, C.K., Velinsky, D.J., Point, D., Benoit, C., Amouroux, D., Plaa, D. and Donard, O.F.X., 2006. Marsh sediments as records of sedimentation, eutrophication and metal pollution in the urban Delaware Estuary. Marine Chemistry, 102(1-2): 72-95.

Coch, N.K., Barton, K.G. and Longoria, A.G., 1991. Holocene Evolution of the Hudson River Estuary. Journal of Coastal Research, SI 11: 55-71.

Coch, N.K. and Bokuniewicz, H., 1986. Oceanographic and Geologic Framework of the Hudson System. Northeastern Geology, 8(3): 96-108.

Cutshall, N.H., Larsen, I.L. and Olsen, C.R., 1983. Direct analysis of Pb-210 in sediment samples - Self-absorption corrections. Nuclear Instruments and Methods, 206(1-2): 309-312.

Dean, W.E., 1974. Determination of Carbonate and Organic Matter in Calcareous Sediments and Sedimentary Rocks by Loss on Ignition: Comparison With Other Methods. Journal of Sedimentary Petrology, 44(1): 242-248.

Feng, H., Cochran, J.K., Hirschberg, D.J. and Wilson, R.E., 1998. Small-scale spatial variations of natural radionuclide and trace metal distributions in sediments from the Hudson River estuary. Estuaries, 21(2): 263-280.

Fountain, K., 2003. The Concept of an Equilibrium Profile and the Effect of Dredging on Sedimentation in Two Reaches of the Hudson River Estuary. M.A. Thesis, Columbia University, New York, 20 pp.

Geyer, W.R., 1993. The Importance of Suppression of Turbulence by Stratification on the Estuarine Turbidity Maximum. Estuaries, 16(1): 113-125.

Geyer, W.R., Signell, R.P. and Kineke, G.C., 1998. Lateral trapping of sediment in a partially mixed estuary. In: Dronkers and Scheffers (Editors), Physics of Estuaries and Coastal Seas. Balkema, Rotterdam, pp. 115-124.

Geyer, W.R., Woodruff, J.D. and Traykovski, P., 2001. Sediment Transport and Trapping in the Hudson River Estuary. Estuaries, 24(5): 670-679.

Hagen, R.A. and Vogt, P.R., 1999. Seasonal variability of shallow biogenic gas in Chesapeake Bay. Marine Geology, 158: 75-88.

Jaeger, J.M. and Nittrouer, C.A., 1995. Tidal controls on the formation of fine-scale sedimentary strata near the Amazon river mouth. Marine Geology, 125: 259-281.

Klingbeil, A.D. and Sommerfield, C.K., 2005. Latest Holocene evolution and human disturbance of a channel segment in the Hudson River Estuary. Marine Geology, 218(1-4): 135-153.

Krishnaswamy, S., Lal, D., Martin, J.M. and Meybeck, M., 1971. Geochronology of lake sediments. Earth and Planetary Science Letters, 11(1-5): 407-414.

McHugh, C.M.G., Pekar, S.F., Christie-Blick, N., Ryan, W.B.F., Carbotte, S. and Bell, R., 2004. Spatial variations in a condensed interval between estuarine and open-marine settings: Holocene Hudson River estuary and adjacent continental shelf. Geology, 32(2): 169-172.

Newman, W.S., Thurber, D.L., Zeiss, H.S., Rokach, A. and Musich, L., 1969. Late quaternary geology of the Hudson River Estuary: a preliminary report. Transactions of the New York Academy of Sciences, 31(5): 548-569.

Nichols, M.M. and Howard-Strobel, M.M., 1991. Evolution Of An Urban Estuarine Harbor - Norfolk, Virginia. Journal Of Coastal Research, 7(3): 745-757.

Nitsche, F.O., Bell, R., Carbotte, S.M., Ryan, W.B.F., Slagle, A., Chillrud, S., Kenna, T., Flood, R., Ferrini, V., Cerrato, R., McHugh, C. and Strayer, D., 2005. Integrative Acoustic Mapping Reveals Hudson River Sediment Processes and Habitats. EOS, Transactions, American Geophysical Union, 86(24): 225, 229.

Nitsche, F.O., Bell, R.E., Carbotte, S.M., Ryan, W.B.F. and Flood, R., 2004. Process-related classification of acoustic data from the Hudson River Estuary. Marine Geology, 209(1-4): 131-145.

Nitsche, F.O., Ryan, W.B.F., Carbotte, S.M., Bell, R.E., Slagle, A., Bertinado, C., Flood, R., Kenna, T. and McHugh, C., 2007. Regional patterns and local variations of sediment distribution in the Hudson River Estuary. Estuarine, Coastal, and Shelf Sciences, 71(1-2): 259-277.

Olsen, C.R., Larsen, I.L., Mulholland, P.J., Vondamm, K.L., Grebmeier, J.M., Schaffner, L.C., Diaz, R.J. and Nichols, M.M., 1993. The concept of an equilibrium surface applied to particle sources and contaminant distributions in estuarine sediments. Estuaries, 16(3B): 683-696.

Olsen, C.R., Simpson, H.J., Bopp, R.F., Williams, S.C., Peng, T.H. and Deck, B.L., 1978. A geochemical analysis of the sediments and sedimentation in the Hudson Estuary. Journal of Sedimentary Petrology, 48(2): 401-418.

Olsen, C.R., Simpson, H.J., Peng, T.H., Bopp, R.F. and Trier, R.M., 1981. Sediment mixing and accumulation rate effects on radionuclide depth profiles in Hudson estuary sediments. Journal of Geophysical Research-Oceans and Atmospheres, 86(C11): 11020-11028.

Pettofrezzo, A.J., 1978. Matrices and Transformations. Dover Publications, New York.

Slagle, A.L., Ryan, W.B.F., Carbotte, S.M., Bell, R., Nitsche, F.O. and Kenna, T., 2006. Late-stage estuary infilling controlled by limited accommodation space in the Hudson River. Marine Geology, 232(3-4): 181-202.

Traykovski, P., Geyer, R. and Sommerfield, C., 2004. Rapid sediment deposition and fine-scale strata formation in the Hudson estuary. Journal of Geophysical Research, 109(F2).

Woodruff, J.D., Geyer, W.R., Sommerfield, C.K. and Driscoll, N.W., 2001. Seasonal variation of sediment deposition in the Hudson River estuary. Marine Geology, 179: 105-119.

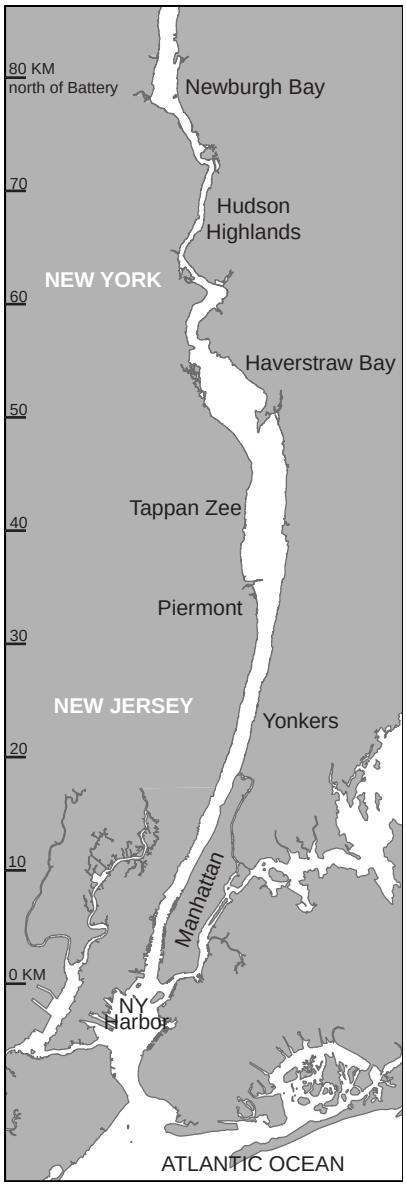

Figure 1. Study area, the lower Hudson River Estuary.

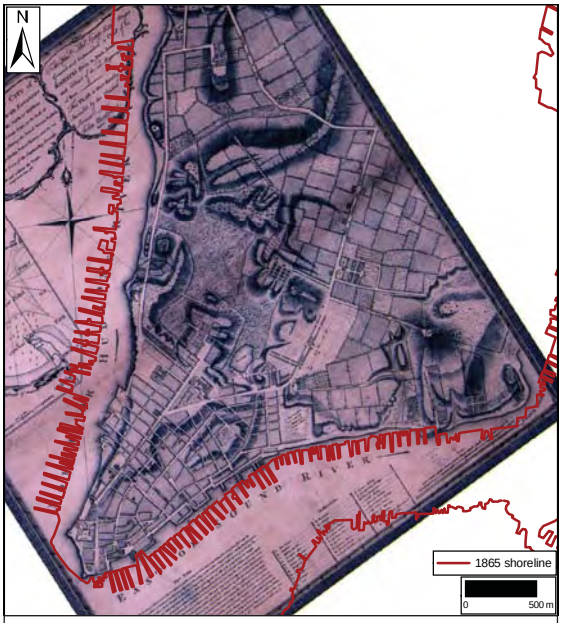

1766 map: A plan of the city of New York and its environs, to Greenwich, on the North or Hudsons River, and to Crown Point, on the west or Sound River, showing the several streets, public buildings, docks, fort, and Battery, surveyed in the winter, 1766. To the honorable Thomas Gage, Esq., major general and commander in chief of his majesty's forces in North America and colonel of the 22nd regiment of foot. This plan is most humbly inscribed by his obedient servant, John Montresor, Engineer.

1776 map: To his excellency Sir Henry Moore, Bart., captain general and governor in chief in and over his majesty's province of New York and the territories depending thereon in America, chancellor and vice admiral of the same. This plan of the city of New York and its environs, surveyed and laid down, is most humbly dedicated by his most obedient servant, B. Ratzer. Surveyed in 1766 and 1767, published 1776.

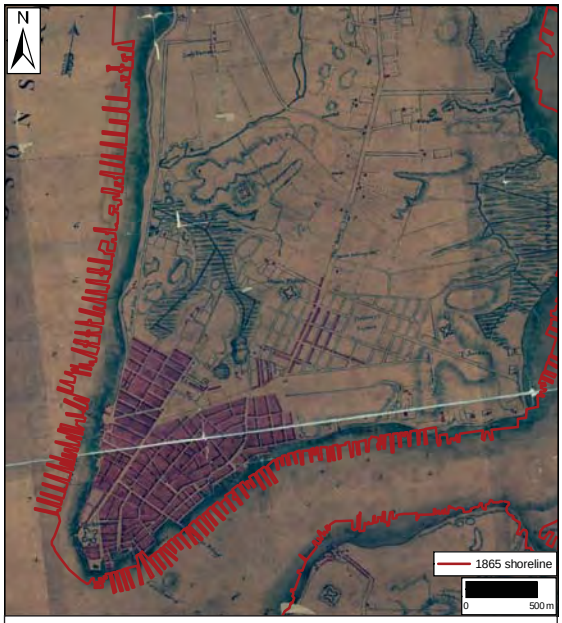

1781 map: Plan de New-York et des îles environnantes. Created/published 1781? Rochambeau collection.

1865 map: Hudson River, Sheet No. 1 From New York to Haverstraw. From a trigonometrical survey under the direction of A.D. Bache, Superintendent of the Survey of the Coast of the United States.

Figure 2. Historic maps of the plan of New York City, at the southwest tip of the island of Manhattan. Red outline shows 1865 shoreline.

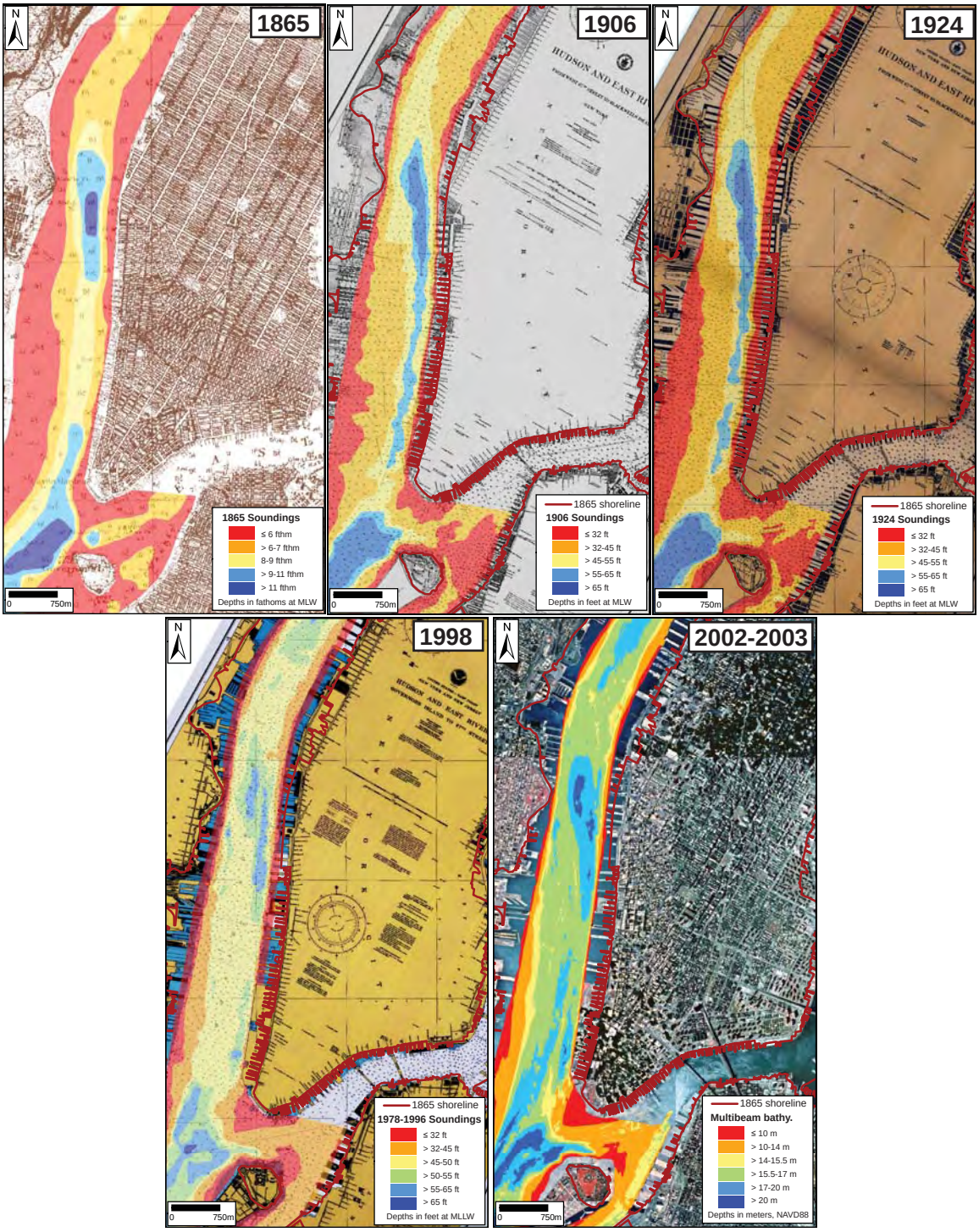

Figure 3. Historic and modern maps of the Manhattan area, showing bathymetric data from the Hudson River estuary between 1865 (upper left panel) and 2003 (lower right panel). Red outline shows 1865 shoreline.

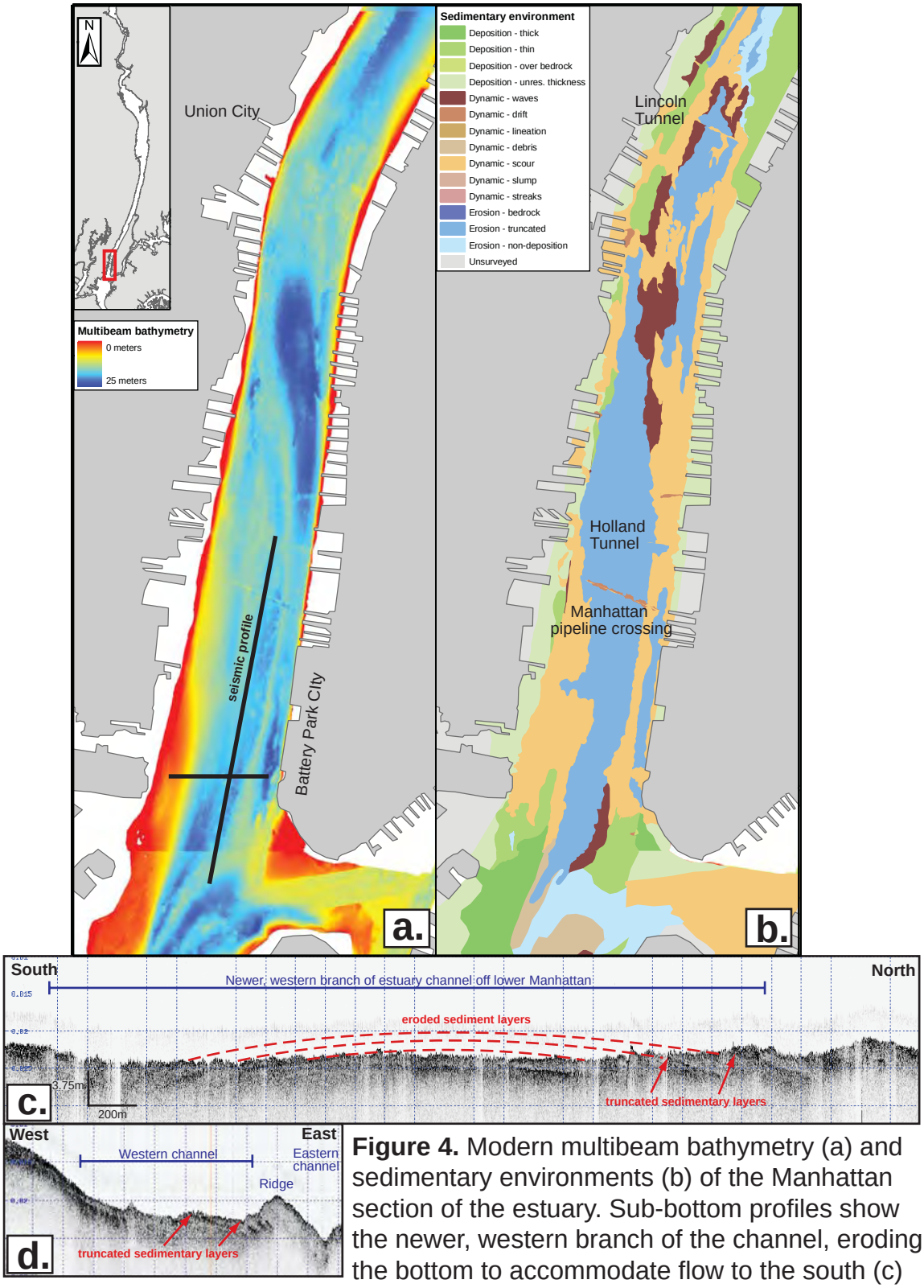

Figure 4. Modern multibeam bathymetry (a) and sedimentary environments (b) of the Manhattan section of the estuary. Sub-bottom profiles show the newer, western branch of the channel, eroding the bottom to accommodate flow to the south (c) and the ridge separating the newer, western channel from the older, eastern branch (d).

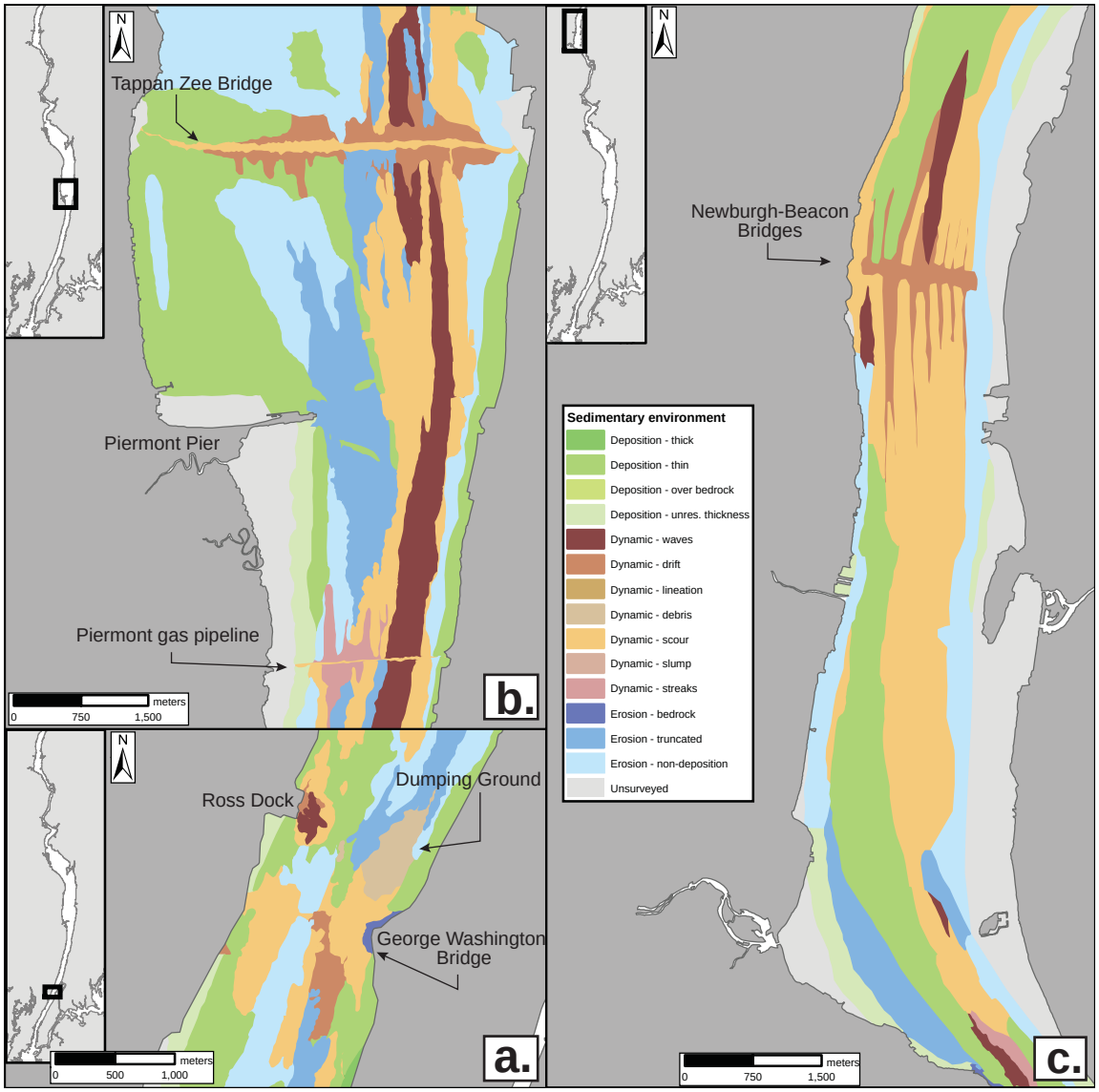

Figure 5. Examples of patterns in sedimentary environment associated with anthropogenic structures in the Manhattan (a), Tappan Zee (b), and Newburgh Bay (c) areas of the Hudson River Estuary.

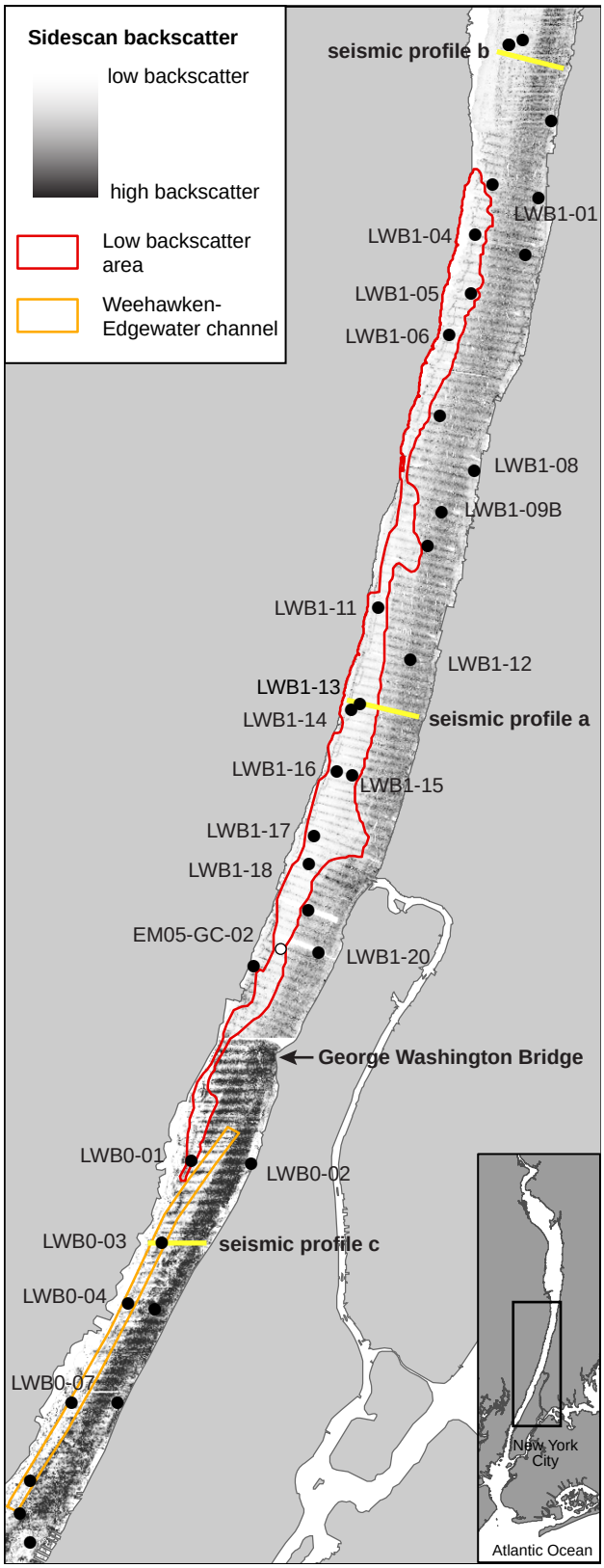

Figure 6. 100kHz sidescan sonar data from the Manhattan-Yonkers stretch. Core locations are shown by circles. Selected cores are labeled; data from these cores appear in Figs. 8-11. Red outline shows low backscatter region along the marginal flats, which may correspond to an acoustically transparent layer of sediment in seismic profiles and cores. Orange outline shows the Weehawken-Edgewater channel, dredged until 1994 by the Army Corps of Engineers. Seismic profiles (a-c), yellow tracks, are shown in Fig. 7.

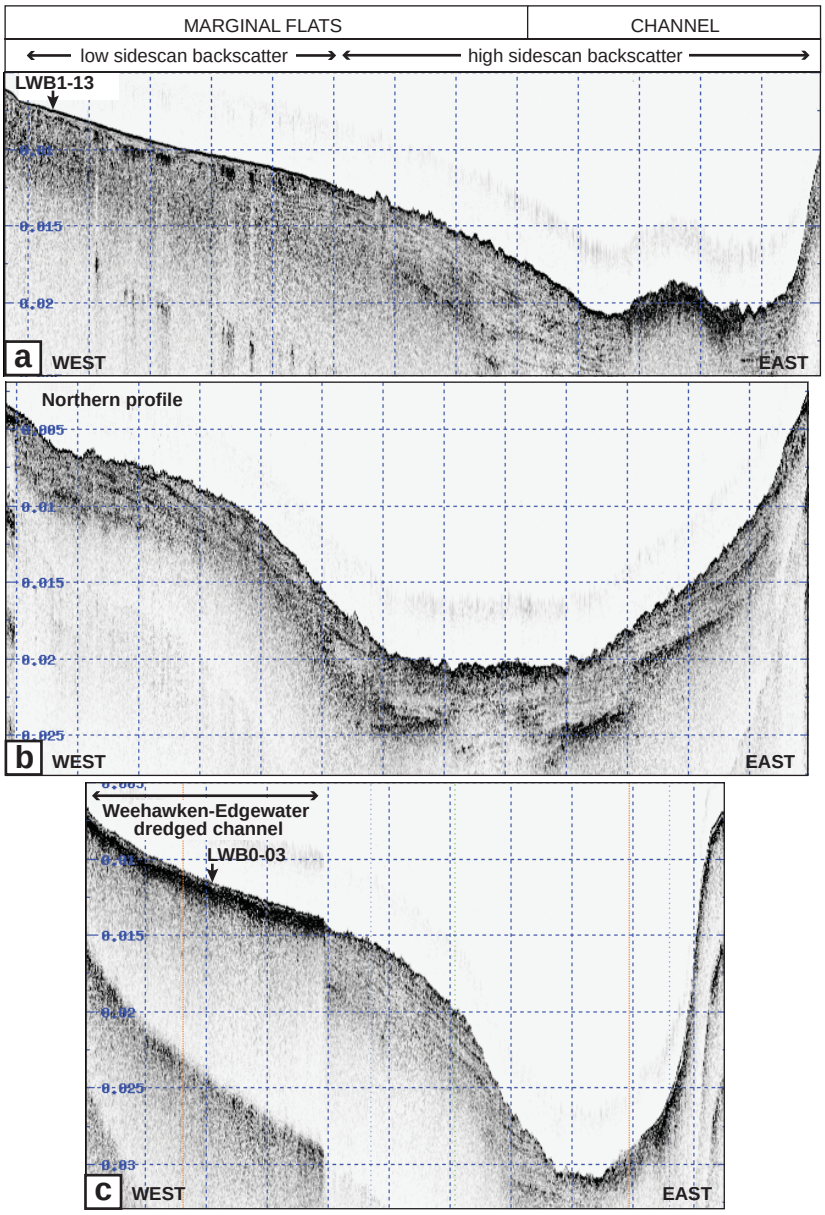

Figure 7. Seismic profiles (a-c) showing bottom morphology and sub-bottom reflections. In profile a, an acoustically-transparent surface layer along marginal flats corresponds to the region of low sidescan backscatter and sediment with a distinct lithology in cores. Profile b, to the north of the low-backscatter area, shows truncated sedimentary layers along the marginal flats. The dredged Weehawken-Edgewater channel, shown in profile c, is associated with a surface layer with abrupt boundaries to the east and west, with acoustic characteristics that prevent imaging deeper sediments on the marginal flats. Profile locations are shown in Fig. 6 and sediment core photographs are shown in Fig. 8a-b.

Marginal flats cores, west of channel

Figure 8a. Photographs from sediment cores obtained in 2003 from the low sidescan backscatter area north of the GWB. See Fig. 6 for core locations.

Figure 8b. Photographs from sediment cores obtained in 2003 from the channel, east bank, and Weehawken-Edgewater dredged channel in the Manhattan to Yonkers stretch of the estuary. See Fig. 6 for core locations.

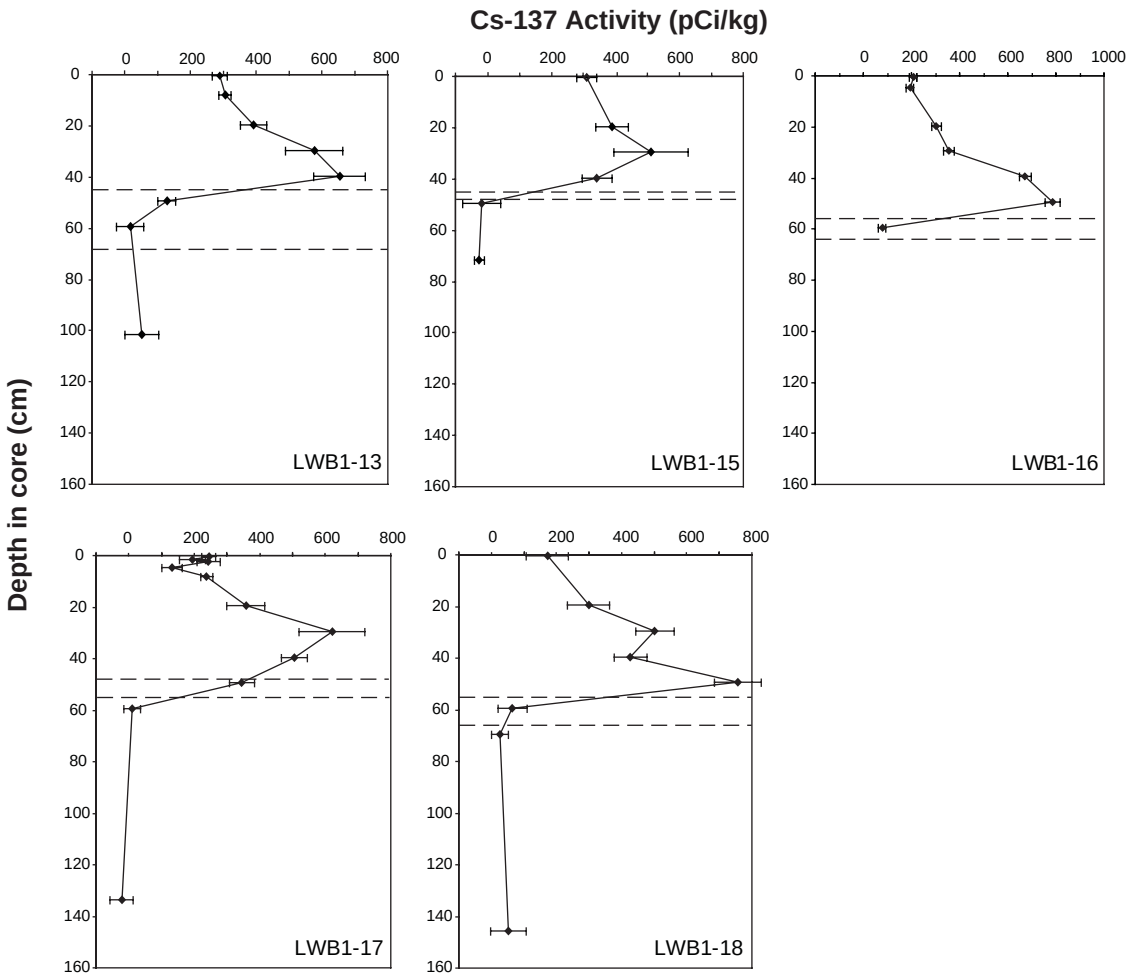

Figure 9. ^{137}Cs activity profiles for cores from the low sidescan backscatter region north of the GWB. Upper dashed lines represent the depth of the black - olive brown sediment boundary; lower dashed lines represent the deepest depth of finger-like intrusions of black mud into the deeper olive brown sediment. See Fig. 6 for core locations.

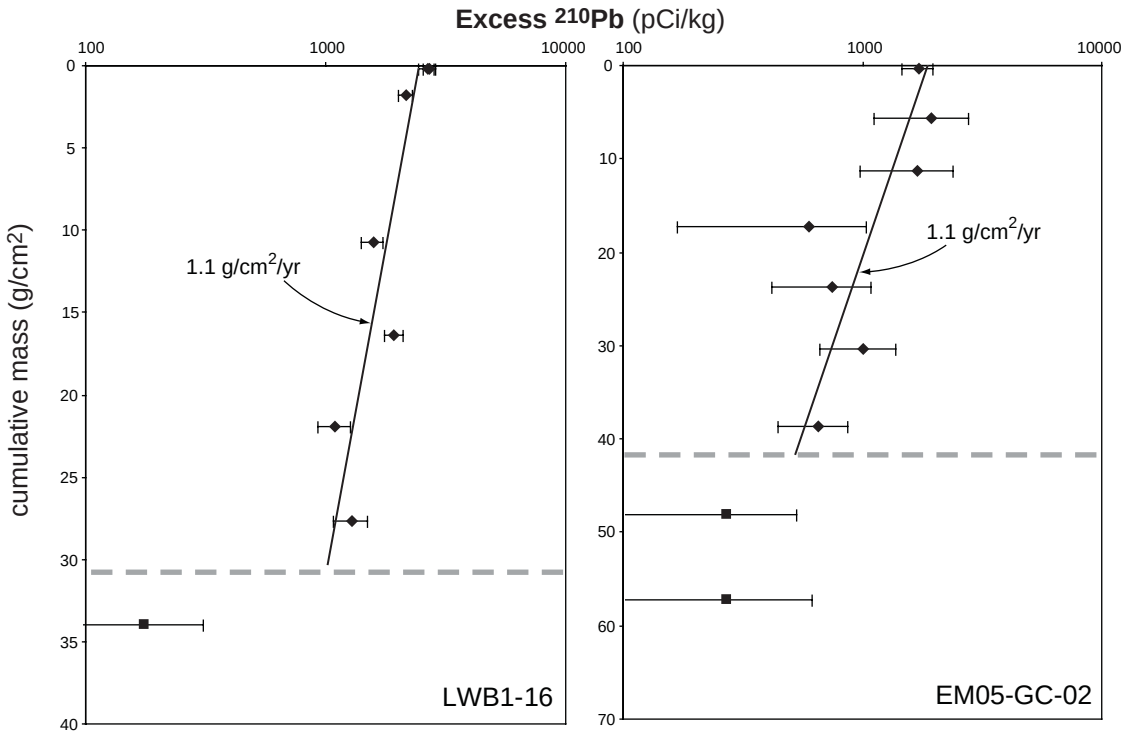

Figure 10. Plots of excess ^{210}Pb activity against cumulative mass for two cores from the low backscatter sidescan area. Diamonds are data points above the lithologic boundary (black mud - olive brown mud boundary, shown as dashed line) and squares show data below the boundary. Solid line is an exponential fit to the data points in the layer with ^{137}Cs and significant excess ^{210}Pb. Core locations are shown in Fig. 6.

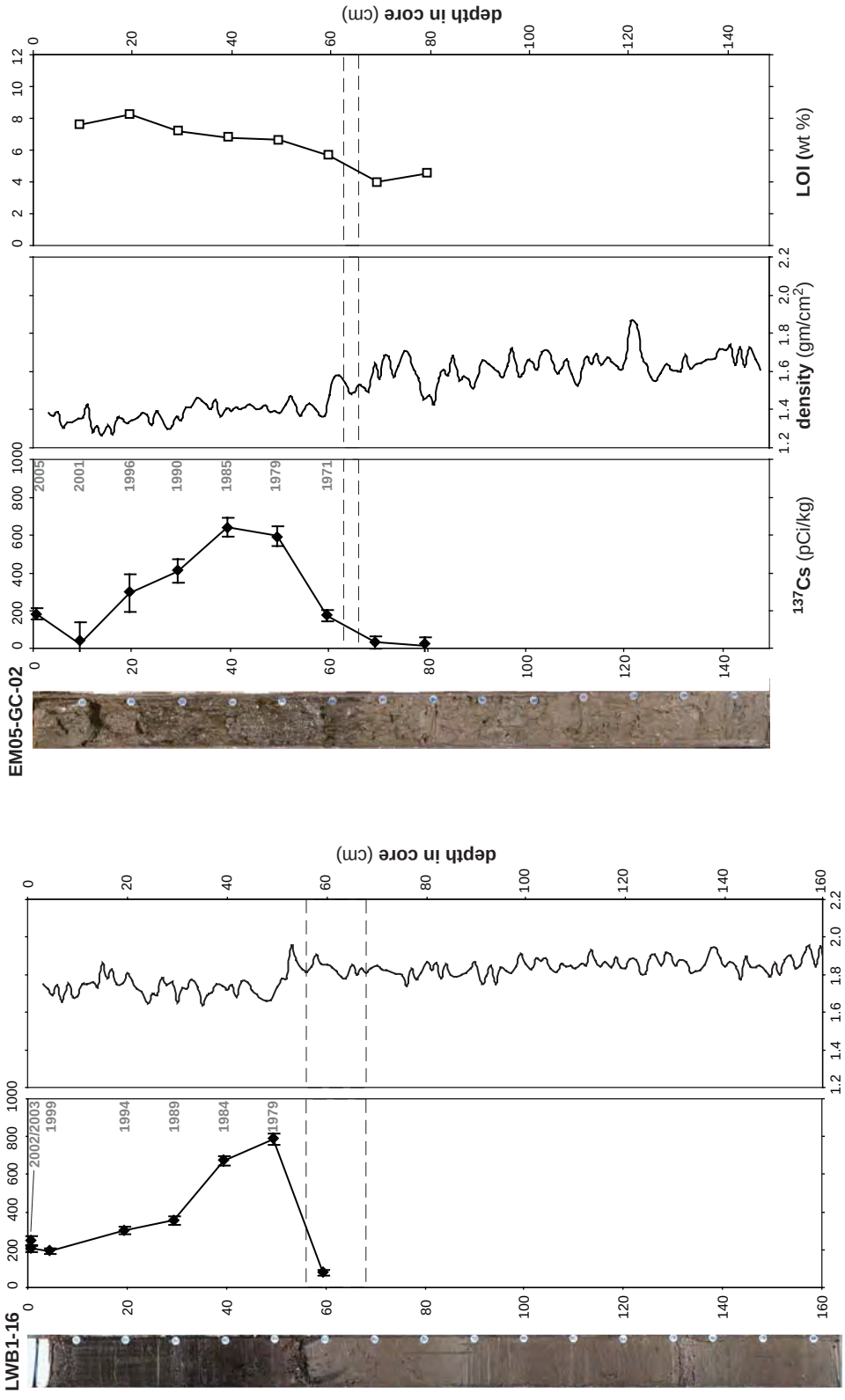

Figure 11. Photographs and profiles of ^{137}Cs, density, and loss-on-ignition (LOI) from cores in the low sidescan backscatter region, showing good agreement between lithological boundaries and change in geochemical and physical properties. The upper and lower horizontal dashed lines mark the boundary and mixed layer depths, respectively. Cumulative-mass adjusted ages, based on sediment accumulation rates from excess ^{210}Pb (Fig. 10), are shown in gray.

Table 1. Historic maps and nautical charts of the New York City area

Date	Title (publisher)	Survey date/s	Source
1766	A plan of the city of New York and its environs (John Montresor, Engineer)	1766	U.S. Library of Congress
1776	A plan of the city of New York and its environs (B. Ratzer)	Hydrography: 1766, 1767	U.S. Library of Congress
1781 [?]	Plan de New-York et des îles environnantes (unk.)	1781?	
1865	Hudson River, Sheet No. 1, From New York to Haverstraw (U.S. Coast Survey Office)	Hydrography: 1854-1856	NOAA OCS
1906	Hudson and East Rivers (U.S. Coast & Geodetic Survey)	Hydrography: 1885, 1889, 1903, 1907	NOAA OCS
1924	Hudson and East Rivers (U.S. Coast & Geodetic Survey)	Hydrography: 1924	NOAA OCS
1998	Hudson and East Rivers (U.S. Coast & Geodetic Survey)	Hydrography: 1978-1996	NOAA OCS

Table 2. Sedimentary environments in the Hudson River estuary (Nitsche et al., 2004)

Sedimentary environment	Geophysical description
Deposition	
Deposition – thin	Low sidescan backscatter, acoustically transparent surface layer in sub-bottom profiles, ≤ 0.5 m thickness
Deposition – thick	Low sidescan backscatter, acoustically transparent surface layer in sub-bottom profiles, > 0.5 m thickness
Deposition – unres. thickness	Low sidescan backscatter, but no or poor-quality sub-bottom data to confirm thickness
Erosion	
Erosion – truncated	Moderate to high sidescan backscatter, sedimentary layers truncated at sediment surface in sub-bottom profiles
Erosion – over bedrock	Bedrock is exposed, no evidence of deposition
Erosion – non-deposition	Moderate to high sidescan backscatter, no clear evidence of recent drape or truncated layers to indicate deposition or clear erosion
Dynamic	
Dynamic – scour	High backscatter, uneven estuary floor, evidence of localized deposition and erosion around obstacles (e.g. bridge pilings) and in channel
Dynamic – waves	Sediment waves in sub-bottom and multibeam bathymetry
Dynamic – debris	Complex morphology in sub-bottom and multibeam, often showing erosion and sediment tails around individual features, often marked as dump sites in navigational charts
Dynamic – drift	Low sidescan backscatter, sediment bodies in sub-bottom and multibeam data, with moderate sidescan backscatter along edges
Dynamic – lineation	Bedforms in multibeam bathymetry oriented parallel to current
Dynamic – streaks	Moderate sidescan backscatter features aligned parallel to current, no evident topographic relief

Table 3. Anthropogenic structures in the lower Hudson River estuary

		km north of Battery
Bridges		
	Newburgh-Beacon Bridges	91
	Tappan Zee Bridge	41
	George Washington Bridge	17
Tunnels		
	Lincoln Tunnel	7.5
	Holland Tunnel	5
Pipeline and Cable Crossings		
	Newburgh pipeline and cable crossing, south of Wappinger's Creek	96
	Newburgh-Beacon Bridges pipeline and cable crossing	89
	Highland Falls cable crossing, south of West Point	75
	Indian Point cable crossing	63
	Stony Point Bay cable crossing	60
	Tappan Zee cable crossing	41
	Piermont Pier pipeline crossing	35
	Riverbank State Park pipeline crossing, off 135th St.	14
	Manhattan pipeline crossing, off 80th St.	10
	Manhattan pipeline crossing, south of Holland Tunnel	2
Dumping Grounds		
	Spuytin Duyvil dumping ground, discontinued	22
	Dumping ground north of George Washington Bridge, discontinued	17.5
Outbuilding Examples		
	Piermont Pier	38
	Ross Dock	18
	Riverbank State Park, off 135th St.	14

Table 4. Extent of sedimentary environments associated with anthropogenic structures

BRIDGES	km from Battery	*Dynamic scour*	*Dynamic drifts*	*Erosion*
Newburgh-Beacon Bridges	91	1400 m cross-est.	1325 m cross-est. Indiv. bridge ribbons: 50-175 m cross-est. 1500-4000 m along-est.	
Tappan Zee Bridge	41	4200 m cross-est. 150 m along-est.	3275 m cross-est. Indiv. bridge ribbons: 75-225 m cross-est. 450-1500 m along-est.	Patchy channel erosion
George Washington Bridge	17	channel: 500 m cross-est. 1800 m along-est. margins: 450 m cross-est. 1200 m along-est.	100-275 m cross-est. 1000 m along-est.	75 m cross-est. 400 m along-est.
TUNNELS	km from Battery	*Dynamic scour, Dynamic waves, Erosion (complex regions)*		
Lincoln Tunnel	7.5	625 m cross-est.		
Holland Tunnel	5	1000 m cross-est. (Dynamic scour and Erosion, only)		
PIPELINES	km from Battery	*Dynamic scour*	*Dynamic drifts*	*Dynamic streaks*
Piermont Pier pipeline	35	1700 m cross-est. 60 m along-est.		700 m cross-est. 425-2000 m along-est.
Manhattan pipeline, 80th St.	10		475 m across-est. 25 m along-est.	
Manhattan pipeline, Holland Tunnel	2	800 m cross-est. 20 m along-est.	750 m cross-est. 30 m along-est.	
DUMPING GDS.	km from Battery	*Dynamic debris*		
Spuytin Duyvil	22	250 m cross-est. 2700 m along-est.		
Dumping ground, GWB	17.5	300 m cross-est. 1050 m along-est.		
OUTBUILDING	km from Battery	*Dynamic scour, Dynamic drifts, Erosion*		
Piermont Pier	38	100-800 m cross-est. 4400 m along-est. (Erosion only)		
Ross Dock	18	100-325 m cross-est. 875 m along-est.		